Dengqiu Ma ✉
Bing Jiang
Zhenhuan Ye
Yongping Liu

https://doi.org/10.21278/TOF.491064724
ISSN 1333-1124
eISSN 1849-1391

DESIGN OPTIMISATION OF THE TOOTH SURFACE OF A VARIABLE HYPERBOLIC CIRCULAR ARC TOOTH TRACE CYLINDRICAL GEAR BASED ON LOADED TRANSMISSION ERROR

Summary

To reduce the vibration and noise of the variable hyperbolic circular arc tooth trace (VH-CATT) cylindrical gear transmission system, a method for modifying the tooth surface with an inclined milling cutter head and a parabolic cutter blade is proposed and the design optimisation of the tooth surface of the VH-CATT cylindrical gear is discussed. Firstly, a modified tooth surface equation was derived, and the tooth surface was reconstructed. Next, a tooth contact analysis model of the VH-CATT cylindrical gear was developed, and the tooth surface gap and flexibility matrix were calculated. An analysis model of the load tooth contact of the VH-CATT cylindrical gear was developed further. Then, a controllable design of the tooth surface mark was proposed, and an optimisation model of the tooth surface was developed and solved by the genetic algorithm. Finally, the tooth surface mark and transmission error experiments were carried out. In this study, the load distribution, the loaded transmission error, the expected cutter inclination angle and optimal modification blade parameters are analysed, and the loaded contact characteristics of the transmission were obtained. Furthermore, the conclusion of the study is verified by experiments. The results of the study will provide a theoretical tool for the high-quality VH-CATT cylindrical gear transmission.

Key words: *variable hyperbolic circular arc tooth trace cylindrical gear, tooth surface modification design, loaded tooth contact analysis; loaded transmission error; tooth surface optimisation; controllable design of tooth surface mark*

1. Introduction

Dynamic meshing performance is one of the most important research topics in the field of gear transmission. Many scholars have carried out research on dynamic characteristics of gears [1-3]. The tooth surface modification technology is used to improve the tooth surface load distribution and regulate the gear dynamic characteristics by changing the geometric characteristics of the tooth surface. This technology is also an important technical means to reduce vibration and noise [4-6]. For example, Jia et al. [7] proposed a tooth modification design method for the vibration reduction in involute helical gears considering the measured load spectrum and the amplitude of the loaded transmission error resulting in a decrease in the

meshing impact of the modified gear. Jiang et al. [8] proposed a design and analysis method for the tooth surface dynamic anti-wear modification to improve the contact performance. The variable hyperbolic circular arc tooth trace (VH-CATT) cylindrical gear is a new cylindrical gear transmission [9]. The main characteristics of the VH-CATT cylindrical gear are that the tooth direction line of the VH-CATT cylindrical gear is an arc line, the tooth profile of the middle cross section is involute, and the other sections are hyperbolic [10-11]. The research shows that the advantages of VH-CATT cylindrical gears are the absence of axial thrust forces, better lubrication conditions, higher bending strengths, and a self-aligning ability [12]. So, the application of the VH-CATT cylindrical gear has great potential and the VH-CATT cylindrical gear is expected to replace conventional involute cylindrical gear transmissions in high-speed and heavy-duty applications [13]. So far, the VH-CATT cylindrical gear has achieved great improvements regarding tooth surface forming methods, contact performance, and manufacturing, i.e. regarding the meshing performance and forming methods in particular.

The results of the research on the tooth surface forming methods of VH-CATT cylindrical gears are as follows. Tseng et al. [14] developed a mathematical model of the tooth surface of cylindrical gears with curvilinear teeth based on a rotary cutter head with double-sided blades and discussed the undercutting condition of this gear. A hobbing method for a cylindrical gear with curvilinear teeth was proposed by Tseng et al. [15-16] and Dai et al. [17], and a mathematical model of the tooth surface was developed based on the hobbing method. A machine tool configuration for the VH-CATT cylindrical gear was proposed by Wu et al. [18-19], and a tooth surface equation with machine tool errors was established. Ma et al. [20] proposed a method for processing the VH-CATT cylindrical gear using a double-sided blade cutter head with inclination, and derived equations of the motion control of each axis for a CNC machine tool. Zheng et al. [21] studied the manufacture and design of noncircular gears with curvilinear teeth and developed a mathematical model of the tooth surface. In addition, Ma et al [10-11], Wei et al [22-23] and Zhao et al [24-25] also established a tooth surface mathematical model of the VH-CATT cylindrical gear based on the double-edged milling method of the large cutter head. To improve the contact characteristics of the VH-CATT cylindrical gear, Ma et al [26-27] proposed an improved double-edged milling method with an inclination angle and established a mathematical model of the tooth surface.

Regarding the meshing performance of the VH-CATT cylindrical gear, Wei et al. [9] established a tooth contact analysis (TCA) method of the VH-CATT cylindrical gear to analyse the influence of the different installation errors and different design parameters on the geometric contact characteristics and sensitivity of the gear pair. Guo et al. [28] established an analytical solution to investigate the influence of different parameters on the contact ellipse of the VH-CATT cylindrical gear. Ma et al. [29] conducted an analysis of the real tooth surface contact of a cylindrical gear pair with curvilinear teeth. Ma et al. [26-27] proposed a design method for modifying the tooth surface to improve the bearing capacity of the VH-CATT cylindrical gear and developed a TCA model to study the influence of the modification parameters on the elliptical contact area and the loaded transmission error. Chen et al. [30] analysed the geometric meshing contact performance of a pinion-modified cylindrical gear pair and studied the influence of the machining parameters on the meshing performance. Luo et al. [31] established a mathematical model for the tooth contact analysis, the loaded tooth contact analysis to calculate most time-varying parameters, and developed a thermo-elastohydrodynamic lubrication model of the VH-CATT cylindrical gear transmission. Wei et al. [22-23] proposed a computing formula for the maximum contact stress of the VH-CATT cylindrical gear according to Hertz formula. Also, by taking the flash contact temperature and the surface roughness in mixed elastohydrodynamic lubrication into account, they integrated a wear prediction model. Another important technical means of the research on contact characteristics is the finite element technology. Fuentes-Aznar et al. [12, 32], Sun et al. [33], and Zhang et al. [34] developed a 3D model of the VH-CATT cylindrical gear to study the contact stress and

bending stress of the VH-CATT cylindrical gear by using the finite element calculation and compared them with the contact characteristics of the straight gear and helical gear. Ma et al. [35-36] proposed the meshing contact impact hypothesis of the VH-CATT cylindrical gear and developed a gear mesh contact impact model to study the VH-CATT cylindrical gear's meshing contact impact properties by the finite element calculation.

VH-CATT cylindrical gears have been researched extensively. However, the above studies on the meshing characteristics of the VH-CATT cylindrical gear mainly focused on the geometric tooth contact analysis. The meshing performance of the VH-CATT cylindrical gear under no load or light load is well understood. However, a finite element technology is used to analyse the load meshing characteristics of the VH-CATT cylindrical gear transmission, although the method involves a large amount of calculation and a single performance index. Also, in reality, especially in heavy load applications, tooth deformation and tooth surface load distribution will have a significant impact on the meshing characteristics of the gear transmissions. In addition, the existing research has failed to yield an active control design and an optimal performance optimisation design of the VH-CATT cylindrical gear. Therefore, there are still some restricting factors in the industrial application of VH-CATT cylindrical gears. For example, the influence of design parameters on the transmission quality of the gear system is not very clear, and so the tooth surface of the VH-CATT cylindrical gear to have an effective reduction in vibration and noise cannot be designed.

In the present study, a method of tooth surface modification is proposed, and the modified tooth surface equation is derived. A mathematical analysis model of the load tooth contact of the VH-CATT cylindrical gear is developed. In this model, the FEM and the linear interpolation method are adopted to determine the comprehensive flexibility matrices of potential contact areas. A controllable design of the tooth surface mark is proposed and a mathematical tooth surface optimisation model is developed. The contact performance of the VH-CATT cylindrical gear is verified by the tooth surface mark and transmission error experiments. Section 2 presents a mathematical model of the modification of the VH-CATT cylindrical gear based on inclined cutter milling and parabolic cutter blade. Section 3 presents a tooth contact analysis model for calculating the tooth surface gap, and the flexibility matrix and linear interpolation are calculated with FEM. Finally, a load tooth contact analysis model is developed, and the load distribution and the load transmission error of the VH-CATT cylindrical gear are obtained. Section 4 proposes a controllable design of the tooth surface mark to calculate the best inclination angle, and a tooth surface optimisation model is developed to calculate the best blade modification parameters. In Section 5, the tooth surface mark and transmission error experiments are carried out to verify the effect of the controllable design of the tooth surface mark and the tooth surface optimisation design for the vibration and noise reduction. The research content provides a technical basis for improving the bearing capacity of the VH-CATT cylindrical gear and optimising the design.

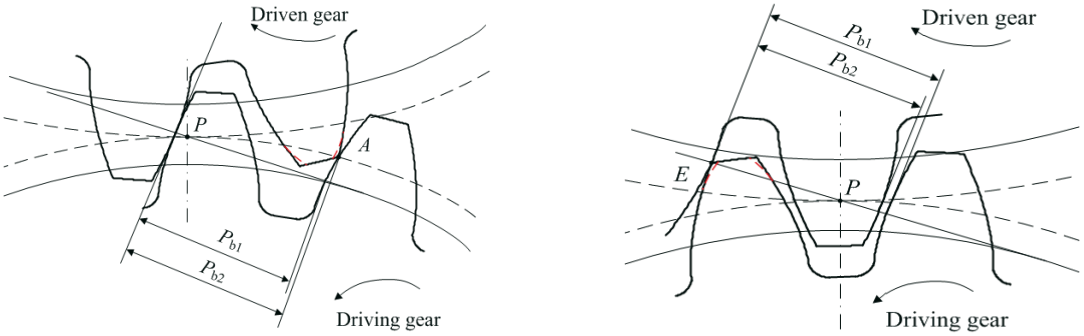
2. Mathematical model of the modification of the VH-CATT cylindrical gear

2.1 Transmission problem of VH-CATT cylindrical gears

Due to the manufacturing and assembly errors in the VH-CATT cylindrical gear transmission, the normal pitch p_{b1} and p_{b2} are not equal, which makes the driven gear accelerate or decelerate instantaneously during meshing transmission, resulting in the meshing impact and vibration of the gear. Fig. 1 shows a meshing impact diagram. In Fig. 1 (*a*), p_{b1} is less than p_{b2}, the latter pair of gear teeth contacts at point A in advance, and the angular velocity of the driven gear increases instantaneously, so that the first pair of gear teeth is out of meshing in advance and the VH-CATT cylindrical gear system generates the impact of mesh-in. In Fig. 1 (*b*), p_{b1} is greater than p_{b2}, when the first pair of gear teeth is out of meshing at point E, the latter pair of gear teeth has not yet entered the meshing, and the VH-CATT cylindrical gear system generates the impact

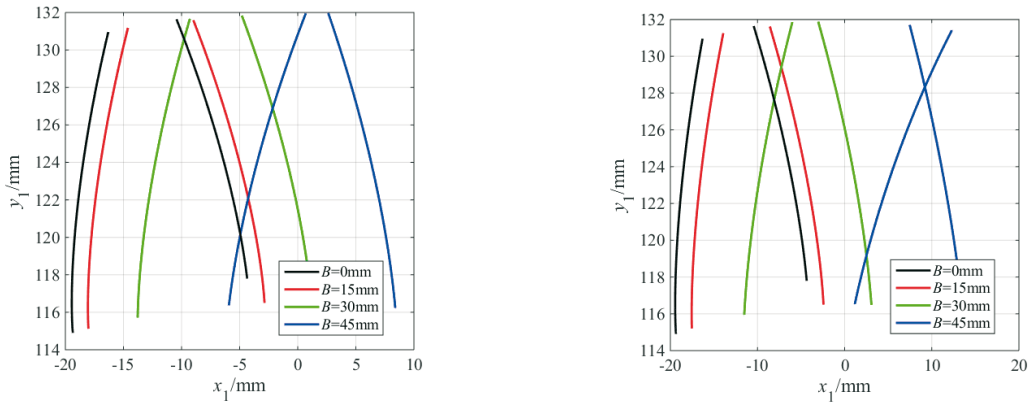
of mesh-out. According to the theory of gear transmission, the main solution to the meshing impact of the VH-CATT cylindrical gear system is a design of the tooth surface modification.

On the other hand, the middle section tooth profile of the VH-CATT cylindrical gear is an involute, and the tooth profile of the other sections is a hyperbola. The tooth thickness gradually decreases from the middle section to the end face, and the tooth profile curve of the concave and convex tooth surfaces shows the trend of '*intersection*' in space. Fig. 2 shows the tooth profile curves of the gear's different sections. Especially when the tooth line radius is smaller, the intersection trend of the tooth profile is more obvious, and the tooth thickness of the gear end face is smaller. At this time, the long axis of the tooth surface contact ellipse reduces and the bearing capacity reduces further. Therefore, the design of the tooth surface modification presented in this paper mainly focuses on the improvement of gear bearing capacity and the reduction in meshing impact.



(*a*) Impact of mesh-in (*b*) Impact of mesh-out

Fig. 1 Meshing impact diagram



(*a*) R_T=80 mm (*b*) R_T=60 mm

Fig. 2 Tooth profile curves of the gear's different sections

2.2 Method of the tooth surface modification and a mathematical model

To improve the bearing capacity of the VH-CATT cylindrical gear, the conventional milling method is abandoned, and the inclined milling method is proposed. To ensure that the pitch line of the cutter blade is tangent to the pitch circle of the gear blank, when the inclined tool is installed as standard, the cutter head is installed at an inclination angle, and the inclination angle is equal to γ. The moving direction of the inclined cutter head is horizontal, as shown in Fig. 3.

To reduce the gear system impact of the meshing-in and meshing-out, a parabolic modification curve is adopted for the tooth profile forming cutter blade, shown in Fig. 3. In O_{dp}-$x_{dp}y_{dp}z_{dp}$, O_{dp} is the parabola vertex position of the parabolic modification curve, u_0 is the distance between the parabola vertex position and the pitch line of the unmodified straight blade. The expression of the parabolic modification curve can be written as:

$$\begin{cases} x_{dp}=u \\ z_{dp}=au^{2n} \end{cases} \tag{1}$$

where a is the parabolic coefficient, the outer blade is positive and the inner blade is negative. n is the parabolic order, n=1, 2, 3 and so on.

The parabolic cutter blade profile in the coordinate system O_{df}-$x_{df}y_{df}z_{df}$ can be written as the coordinate geometric transformation:

$$\begin{cases} x_{df}=\mp\left(u+u_0\right)\sin\alpha\mp\dfrac{\pi m}{4}-au^{2n}\cos\alpha \\ z_{df}=\left(u+u_0\right)\cos\alpha\mp au^{2n}\sin\alpha \end{cases} \tag{2}$$

where the upper part of the symbol is the outer blade and the lower part of the symbol is the inner blade.

To develop a model of a modified tooth surface of the VH-CATT cylindrical gear, the coordinate transformation system of the modified tooth surface is developed based on the inclined cutter milling and parabolic forming cutter blade, shown in Fig. 3. In Fig. 3, v is the moving velocity of the inclined cutter head in the horizontal direction, B is the gear width, R_1 is the pitch circle radius, ω is the angular velocity of the cutter head, ω_1 is the gear blank's angular velocity, m is the gear module of the VH-CATT cylindrical gear, θ_d is the spreading angle of the cutter head, and φ_1 is the involute angle of the tooth profile. O-xyz is the intermediate auxiliary coordinate system, O_d-$x_dy_dz_d$ is the static coordinate system of the inclined cutter, O_{d0}-$x_{d0}y_{d0}z_{d0}$ is the dynamic coordinate system of the inclined cutter, O_1-$x_1y_1z_1$ is the dynamic coordinate system of the gear blank, and O_f-$x_fy_fz_f$ is the static coordinate system of the gear blank.

According to the gear meshing theory [37], the tooth surface equation is the expression of the inclined cutter blade trajectory in the dynamic coordinate system O_1-$x_1y_1z_1$ based on the meshing contact condition. Firstly, the expression of the inclined cutter in the dynamic coordinate system O_d-$x_dy_dz_d$ can be written as Eq. (3) based on Eq. (2), and the coordinate transformation relationship is shown in Fig. 3.

$$\begin{cases} x_d=\left\{\left[\mp\left(u+u_0\right)\sin\alpha\mp\dfrac{\pi m}{4}-au^{2n}\cos\alpha-R_{\mathrm{T}}\right]\cos\gamma+\left[\left(u+u_0\right)\cos\alpha\mp au^{2n}\sin\alpha\right]\sin\gamma\right\}\cos\theta \\ y_d=-\left\{\left[\mp\left(u+u_0\right)\sin\alpha\mp\dfrac{\pi m}{4}-au^{2n}\cos\alpha-R_{\mathrm{T}}\right]\cos\gamma+\left[\left(u+u_0\right)\cos\alpha\mp au^{2n}\sin\alpha\right]\sin\gamma\right\}\sin\theta \\ z_d=-\left[\mp\left(u+u_0\right)\sin\alpha\mp\dfrac{\pi m}{4}-au^{2n}\cos\alpha+R_{\mathrm{T}}\right]\sin\gamma+\left[\left(u+u_0\right)\cos\alpha\mp au^{2n}\sin\alpha\right]\cos\gamma \end{cases} \tag{3}$$

At the same time, according to the inclined cutter equation and the meshing principle, the normal vector of the inclined cutter blade rotation surface at the meshing point can be written as Eq. (4).

$$\begin{aligned} \boldsymbol{n}=&-B\cos\theta\left[\cos\left(\gamma\mp\alpha\right)+2nau^{2n-1}\sin\left(\gamma\mp\alpha\right)\right]\boldsymbol{i}_d+B\sin\theta\left[\cos\left(\gamma\mp\alpha\right)+2nau^{2n-1}\sin\left(\gamma\mp\alpha\right)\right]\boldsymbol{j}_d \\ &+B\left[\sin\left(\gamma\mp\alpha\right)-2nau^{2n-1}\cos\left(\gamma\mp\alpha\right)\right]\boldsymbol{k}_d \end{aligned} \tag{4}$$

where $B=-\left[\mp\left(u+u_0\right)\sin\alpha\mp\dfrac{\pi m}{4}-au^{2n}\cos\alpha-R_{\mathrm{T}}\right]\cos\gamma-\left[\left(u+u_0\right)\cos\alpha\mp au^{2n}\sin\alpha\right]\sin\gamma$.

Secondly, to obtain the mathematical model of the modified tooth surface, the relative velocity of the contact point between the tool and the tooth surface is required. According to references [26] and [37], the relative speed at the meshing point is given in Eq. (5).

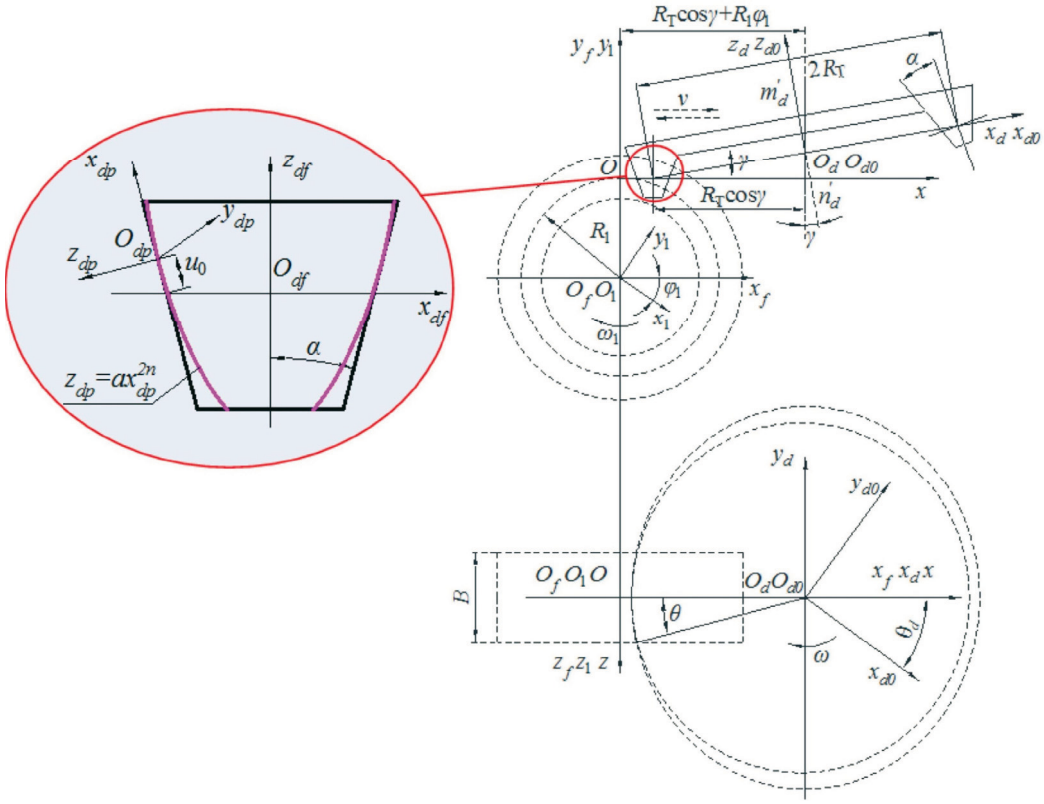


Fig. 3 Forming of tooth surface of the modified gear and the blade of the modified tooth profile

$$\begin{aligned}\boldsymbol{v}=&\left[-(u+u_0)\cos(\gamma\mp\alpha)+\left(R_T\mp\frac{\pi m}{4}+R_1\varphi_1\right)\sin\gamma-au^{2n}\sin(\gamma\mp\alpha)\right]\omega_1\boldsymbol{i}_d+\left\{\left[(u+u_0)\cdot\right.\right.\\&\left.\left.\sin(\gamma\mp\alpha)-\left(R_T\pm\frac{\pi m}{4}\right)\cos\gamma-au^{2n}\cos(\gamma\mp\alpha)\right]\cos\theta+(R_T+R_1\varphi_1\cos\gamma)\right\}\omega_1\boldsymbol{k}_d\end{aligned}\tag{5}$$

Thirdly, according to reference [37], the product of the relative speed and normal vector is zero, namely:

$$\boldsymbol{n}\cdot\boldsymbol{v}=0\tag{6}$$

Eq. (7) is simplified by Eq. (6) and u is the solution of Eq. (7).

$$A_nu^{4n-1}+R_nu^{2n-1}+P_nu+Q_n=0\tag{7}$$

where

$$A_n=2na^2\cos\theta\tag{8}$$

$$\begin{aligned}R_n=&\pm2na\frac{\pi m}{4}\cos\theta\cos\alpha+2naR_T\cos\theta\cos(\gamma\mp\alpha)\\&-2na(R_T+R_1\varphi_1\cos\gamma)\cos(\gamma\mp\alpha)-2naR_1\varphi_1\sin\gamma\cos\theta\sin(\gamma\mp\alpha)\end{aligned}\tag{9}$$

$$P_n=\cos\theta\tag{10}$$

$$\begin{aligned}Q_n=&u_0\cos\theta+\frac{\pi m}{4}\cos\theta\sin\alpha-R_1\varphi_1\sin\gamma\cos\theta\cos(\gamma\mp\alpha)\\&+(R_T+R_1\varphi_1\cos\gamma)\sin(\gamma\mp\alpha)-R_T\cos\theta\sin(\gamma\mp\alpha)\end{aligned}\tag{11}$$

Because Eq. (7) has only one real root and 4n-2 virtual roots, the real root is taken as u value based on the structural characteristics and actual physical significance of the VH-CATT cylindrical gear.

Finally, to get a mathematical model of the modified tooth surface of the VH-CATT cylindrical gear, it is necessary to transform Eq. (3) from O_d-$x_dy_dz_d$ to O_1-$x_1y_1z_1$. According to Fig. 3, the transformation matrix A_{1d} from O_d-$x_dy_dz_d$ to O_1-$x_1y_1z_1$ is obtained in Eq. (12):

$$A_{1d}=\begin{bmatrix} \cos(\gamma+\varphi_1) & 0 & -\sin(\gamma+\varphi_1) & (R_T\cos\gamma+R_1\varphi_1)\cos\varphi_1-R_T\sin\varphi_1\sin\gamma-R_1\sin\varphi_1 \\ \sin(\gamma+\varphi_1) & 0 & \cos(\gamma+\varphi_1) & (R_T\cos\gamma+R_1\varphi_1)\sin\varphi_1+R_T\cos\varphi_1\sin\gamma+R_1\cos\varphi_1 \\ 0 & -1 & 0 & 0 \\ 0 & 0 & 0 & 1 \end{bmatrix} \tag{12}$$

Therefore, the modified tooth surface equation can be expressed as:

$$\begin{cases} x_1^n=\left[(u+u_0)\sin(\gamma\mp\alpha)-au^{2n}\cos(\gamma\mp\alpha)-R_T\mp\dfrac{\pi m}{4}\cos\gamma\right]\cos\theta\cos(\gamma+\varphi_1) \\ \quad -\left[(u+u_0)\cos(\gamma\mp\alpha)+au^{2n}\sin(\gamma\mp\alpha)\pm\dfrac{\pi m}{4}\sin\gamma\right]\sin(\gamma+\varphi_1) \\ \quad +(R_T\cos\gamma+R_1\varphi_1)\cos\varphi_1-R_T\sin\varphi_1\sin\gamma-R_1\sin\varphi_1 \\ y_1^n=\left[(u+u_0)\sin(\gamma\mp\alpha)-au^{2n}\cos(\gamma\mp\alpha)-R_T\mp\dfrac{\pi m}{4}\cos\gamma\right]\cos\theta\sin(\gamma+\varphi_1) \\ \quad +\left[(u+u_0)\cos(\gamma\mp\alpha)+au^{2n}\sin(\gamma\mp\alpha)\pm\dfrac{\pi m}{4}\sin\gamma\right]\cos(\gamma+\varphi_1) \\ \quad +(R_T\cos\gamma+R_1\varphi_1)\sin\varphi_1+R_T\cos\varphi_1\sin\gamma+R_1\cos\varphi_1 \\ z_1^n=\left[(u+u_0)\sin(\gamma\mp\alpha)-au^{2n}\cos(\gamma\mp\alpha)-R_T\mp\dfrac{\pi m}{4}\cos\gamma\right]\sin\theta \end{cases} \tag{13}$$

where n is an integer such as 1, 2, and 3, and it corresponds to the 2nd, 4th and 6th order parabolic modified tooth surface equations, respectively.

3. Analysis model of the load tooth contact of the VH-CATT cylindrical gear

The load tooth contact analysis (LTCA) is an important technical means for the analysis of dynamic performance of the gear transmission system, and it is a bridge between the gear geometry design and gear performance analysis. The key technologies in LTCA numerical calculation include a 3D model, flexibility matrix, tooth surface gap, and a solution of the LTCA model. In this paper, the tooth surface point cloud of the VH-CATT cylindrical gear was obtained based on Eq. (13), it was then used for the reconstruction of the tooth surface, and the flexibility matrix was obtained based on the 3D model. Also, an analysis model of the tooth contact was developed to obtain the tooth surface gap and contact points. Finally, an LTCA model was developed to calculate the load distribution and the load transmission error (LTE).

3.1 Tooth surface gap

Fig. 4 shows the meshing transmission system of the VH-CATT cylindrical gear: Σ^{I} is the driving gear tooth surface, Σ^{II} is the driven gear tooth surface, M is the contact point of the tooth surface, $\boldsymbol{n}_c$ is the common normal vector of the contact point, ψ_1 is the meshing angle of the driving gear, and ψ_2 is the meshing angle of the driven gear. Since the tooth surface is a continuous tangent, the driving gear and the driven gear have the same position vector and a common normal vector at the meshing point in the same coordinate system. If the coordinate system O_g-$X_gY_gZ_g$ is taken as the calculation fixed coordinate system, the same position vector and common normal vector at the meshing point can be expressed as Eq. (14). Eq. (14) is also called a tooth contact analysis model.

$$\begin{cases} \boldsymbol{r}_g^1\left(\theta_1,\varphi_1,\psi_1\right)=\boldsymbol{r}_g^2\left(\theta_2,\varphi_2,\psi_2\right) \\ \boldsymbol{n}_g^1\left(\theta_1,\varphi_1,\psi_1\right)=\boldsymbol{n}_g^2\left(\theta_2,\varphi_2,\psi_2\right) \end{cases} \tag{14}$$

where $\boldsymbol{r}_g^1$ is the driving gear tooth surface, $\boldsymbol{r}_g^2$ is the driven gear tooth surface, $\boldsymbol{n}_g^1$ is the driving gear tooth surface normal vector, and $\boldsymbol{n}_g^2$ is the driven gear tooth surface normal vector.

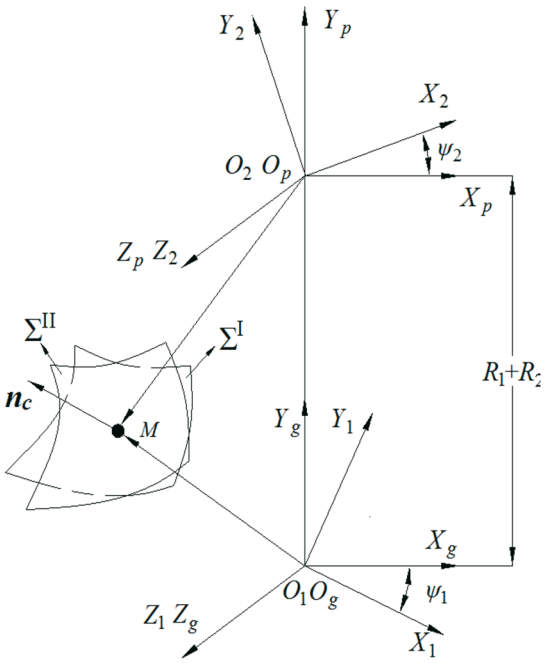


Fig. 4 Meshing transmission system of VH-CATT cylindrical gear

The tooth surface gap mainly includes tooth surface normal gap b and tooth surface initial gap δ. Fig. 5 shows the calculation principle of the gear surface normal gap of the VH-CATT cylindrical gear. In the coordinate system O_g-$X_gY_gZ_g$, $\boldsymbol{r}_g^M$ is the position vector of the contact point, $\boldsymbol{E}_M\boldsymbol{G}_M$ ($\boldsymbol{\xi}_e$) is the direction vector of the contact ellipse long axis, $\boldsymbol{n}_g^M$ is the common normal vector, C_MD_M and A_MB_M are the intersection curves on the tooth surface of the driven gear and driving gear respectively, M^j is a discrete point on the contact ellipse long axis, L is a line parallel to $\boldsymbol{n}_g^M$ and it passes through the M^j point, M_g^j is the intersection point of L on the driving gear surface, M_p^j is the intersection point of L on the driven gear surface, and j is the number of discrete points. The expression of the straight line equation L is Eq. (15).

$$\frac{x_L-x_g^{M^j}}{\boldsymbol{n}_{gx}^M}=\frac{y_L-y_g^{M^j}}{\boldsymbol{n}_{gy}^M}=\frac{z_L-z_g^{M^j}}{\boldsymbol{n}_{gz}^M} \tag{15}$$

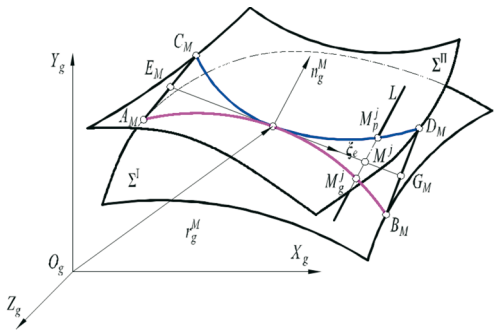


Fig. 5 Calculation principle of gear surface normal gap of VH-CATT cylindrical gear

The coordinates of the intersection points M_g^j and M_p^j can be obtained by combining the straight line equation and the tooth surface equation. It is assumed that the expressions of the intersection points M_g^j and M_p^j are $\left(x_g^{M_g^j}, y_g^{M_g^j}, z_g^{M_g^j}\right)$ and $\left(x_g^{M_p^j}, y_g^{M_p^j}, z_g^{M_p^j}\right)$, and the coordinate expressions are the functions of the θ_1, φ_1 and θ_2, φ_2, respectively. The tooth surface normal gap is the distance from M_g^j to M_p^j. Therefore, the expression of the tooth surface normal gap can be represented as:

$$b_M = \sqrt{\left(x_g^{M_p^j} - x_g^{M_g^j}\right)^2 + \left(y_g^{M_p^j} - y_g^{M_g^j}\right)^2 + \left(z_g^{M_p^j} - z_g^{M_g^j}\right)^2} \tag{16}$$

As for the tooth surface initial gap, it depends on the geometric transmission error, and it is the normal direction displacement of the tooth surface. According to reference [38], Eq. (17) is the expression of the geometric transmission error:

$$\Delta\varphi_2 = \varphi_2(\varphi_{11}) - \varphi_2(\varphi_{110}) - \frac{z_1}{z_2}(\varphi_{11} - \varphi_{110}) \tag{17}$$

where φ_{110} is the initial angular displacement of the driving gear, $\varphi_2(\varphi_{110})$ is the initial angular displacement of the driven gear, φ_{11} is the angular displacement of the driving gear at a certain time, $\varphi_2(\varphi_{11})$ is the angular displacement of the driven gear at a certain time, z_1 is the tooth number of the driving gear, and z_2 is the tooth number of the driven gear.

Therefore, the gear tooth surface gap before loading deformation is $w=b+\delta$.

3.2 Flexibility matrix

The flexibility matrix is a key technology in the LTCA model and it reflects the ability of the tooth surface to resist the deformation of the external load. Based on the 3D model, ABAQUS and Python language, a finite element model is developed to calculate the deformation of the tooth surface discrete points under the unit normal load, and the flexibility matrix is calculated by the interpolation calculation. In the finite element calculation, the unit normal load is applied to the tooth surface discrete point i ($i = 1, 2, 3, \cdots, n$) in turns, and the normal deformation of all discrete points on the tooth surface is extracted in turns, and then the flexibility matrix of the tooth surface discrete point is obtained.

However, the LTCA calculation needs a contact point flexibility matrix. But it is difficult to achieve complete coincidence between the discrete contact points and the tooth surface discrete points, so the only solution is the interpolation calculation. To simplify the interpolation calculation of the flexibility matrix, the tooth surface discrete points and contact points are transferred to the cross section of the rotating gear shaft. Namely, *x*, *y*, and *z* coordinates are transformed into the *r* and *z* coordinates, and $r = \sqrt{x^2 + y^2}$. Fig. 6 shows a schematic diagram of the calculation principle of the contact point flexibility matrix. In Fig. 6, ○ is the tooth surface discrete point, ⊙ is the instantaneous contact point, and ● is the tooth surface node of the interpolation area.

The first step of the interpolation calculation is calculating the equivalent load of the interpolation area points F_i.

The second step of the interpolation calculation is calculating the normal deformation of the whole tooth surface under an equivalent load at p_i point in turns.

The third step of the interpolation calculation is calculating the normal deformation of each contact point by interpolation.

The final step of the interpolation calculation is calculating the flexibility coefficient of the contact point M_c by linear superposition.

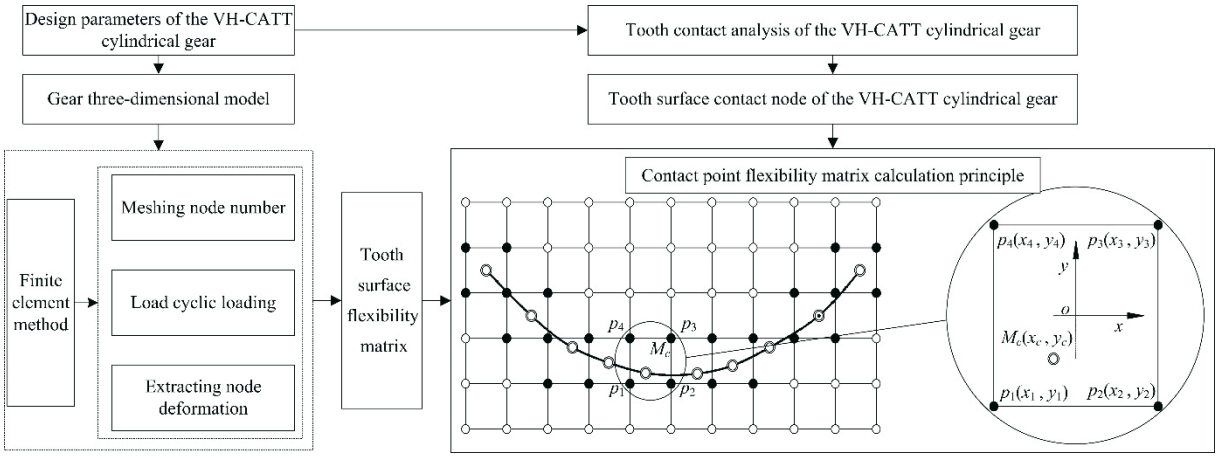


Fig. 6 Calculation principle of contact point flexibility matrix

3.3 Load tooth contact analysis model

According to reference [38], the deformation compatibility equation at any contact point j can be expressed as:

$$\left(\sum_{k=1}^{n} f_{jk} + \sum_{k=1}^{n} f_{j'k'}\right) F_k + w_j = s_z + d_j \tag{18}$$

where d_j is the remaining gap of the tooth surface if d_j=0, $F_j > 0$ or if $d_j > 0$, $F_j = 0$, f_{jk} and $f_{j'k}$ are the flexibility coefficients of the driving gear and the driven gear, respectively. w_j is the tooth surface gap of j point, F_k is the load at k point, and s_z is the normal displacement of the driven gear under external load.

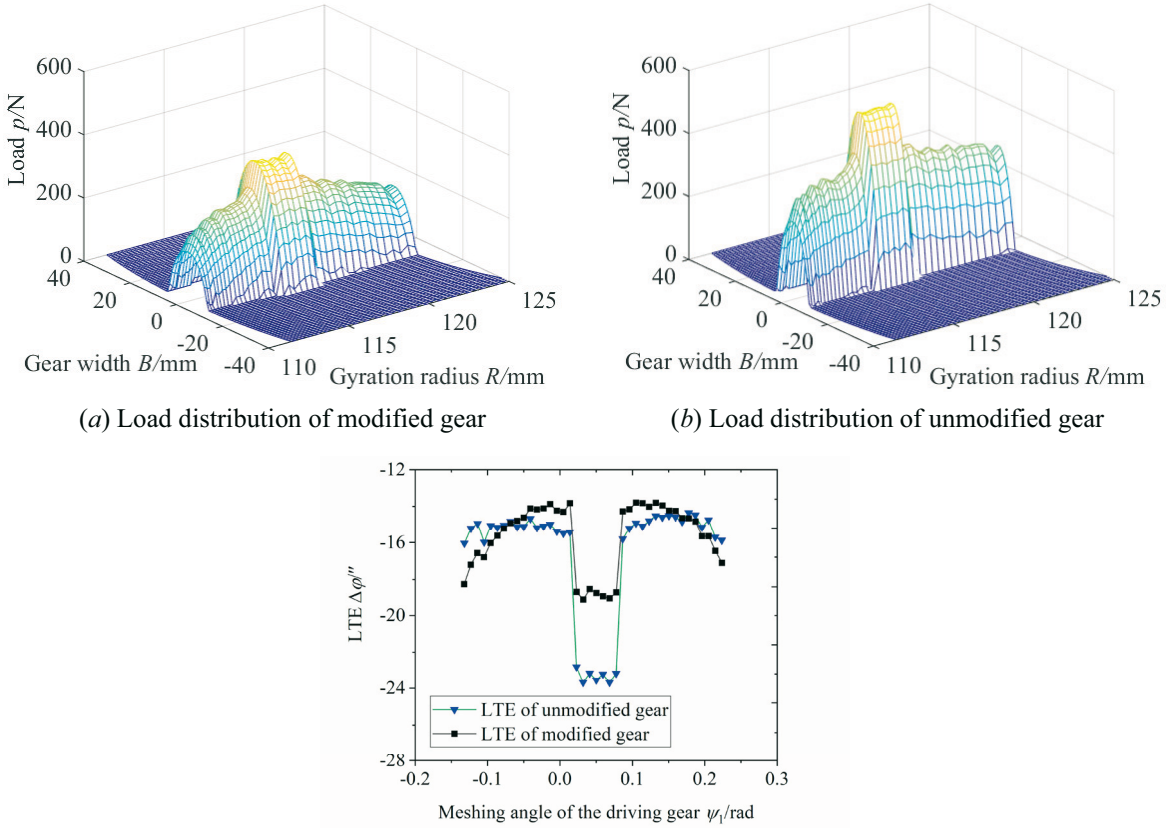
According to reference [38] and based on the conditions of deformation coordination, force balance, and non-embedding, the following mathematical model is established to describe the equilibrium state of the tooth contact under load:

$$\begin{cases} f = \min\left[\dfrac{1}{2}\left(\boldsymbol{P}^T \boldsymbol{S}\right)\boldsymbol{P}\right] \\ [w]_m = -[S]_m [F]_m + s_z [e] + [d]_m, m = \mathrm{I}, \mathrm{II} \\ T = \sum_{i=0}^{n}\left(\boldsymbol{d}_{i\mathrm{I}}\boldsymbol{n}_{\mathrm{I}}\boldsymbol{F}_{i\mathrm{I}} + \boldsymbol{d}_{i\mathrm{II}}\boldsymbol{n}_{\mathrm{II}}\boldsymbol{F}_{i\mathrm{II}}\right) \\ S.t: d_j > 0\left(d_j = 0\right) \| F_j = 0\left(F_j > 0\right), s_z \geq 0, F_j \geq 0 \end{cases} \tag{19}$$

where $\boldsymbol{P}$ is the tooth surface load, and $\boldsymbol{P}$=[$\boldsymbol{F}_{\mathrm{I}}$;$\boldsymbol{F}_{\mathrm{II}}$]. $j = 1, 2, 3, \cdots, 2n$, I, II represent the first and second pairs of teeth, respectively, [S] is the flexibility matrix of the tooth contact point, $\boldsymbol{S}$=[$\boldsymbol{S}_{\mathrm{I}}$ 0;0 $\boldsymbol{S}_{\mathrm{II}}$], [$F$] is the load matrix of the tooth contact point, [w] is the initial clearance matrix, [d] is the residual clearance matrix, $\boldsymbol{n}_{\mathrm{I}}$ and $\boldsymbol{n}_{\mathrm{II}}$ are the unit normal vectors of the first and second pairs of teeth, $\boldsymbol{d}_{i\mathrm{I}}$ and $\boldsymbol{d}_{i\mathrm{II}}$ are the matrixes composed of the rotation radius of discrete points on the contact line, and [e] is the unit diagonal matrix.

3.4 Numerical example

According to the LTCA model, the tooth surface load and the load transmission error are calculated. Fig. 7 shows the load distribution and the load transmission error of the VH-CATT cylindrical gear, the load T=1000 N·m, and the main parameters are as follows: modulus m=8 mm, pressure angle α=20°, gear numbers z_1=29 and z_2=41, tooth line radius R_T=200 mm, parabolic coefficient a=–0.00005, parabolic vertex position u_0=0 mm, cutter head inclination angle γ=5°. According to Fig. 7, the load of the modified tooth surface is obviously smaller than that of the unmodified tooth surface, and the load mutation in the alternate area of the single and double tooth meshing decreases. Also, the load transmission error increases at the moment of meshing-in and out, but the amplitude of the load transmission error and the amplitude of the load transmission error in the alternating area of the single and double teeth meshing decrease. The research shows that the tooth surface modification design is beneficial in reducing the vibration and noise of the VH-CATT cylindrical gear.



(*a*) Load distribution of modified gear

(*b*) Load distribution of unmodified gear

(*c*) Load transmission error

Fig. 7 Load distribution and load transmission error of VH-CATT cylindrical gear

4. Design optimisation of the tooth surface of the VH-CATT cylindrical gear

4.1 Controllable design of the tooth surface mark

Because the tooth thickness gradually decreases from the middle section to the end face, the tooth profile curve of the concave and convex tooth surfaces shows the trend of '*intersection*' in space. The long axis of the contact ellipse is small, especially when the tooth line radius is small. Therefore, a method of forming the tooth surface with an inclined cutter head is proposed to increase the contact area and improve the bearing capacity of the VH-CATT cylindrical gear. However, in gear transmission, the long axis size of the tooth surface contact ellipse and the

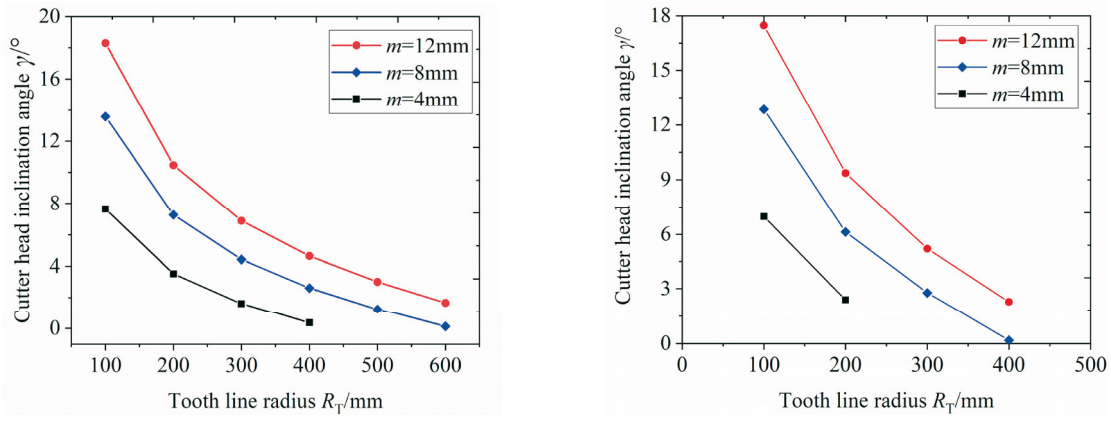
sensitivity of the system installation errors pose a contradictory problem. When the long axis of the tooth surface contact ellipse is small, the gear system is less sensitive to installation errors, but the bearing capacity of the gear pair is also low. When the long axis of the tooth surface contact ellipse is large, the bearing capacity of the gear pair system is large, but the sensitivity to installation errors is also large. The tooth profile modification design method based on the inclined cutter head can effectively increase the length of the instantaneous contact ellipse and improve the bearing capacity, but the long axis of the instantaneous contact ellipse cannot be increased to the tooth width. Therefore, to accurately control the tooth surface mark, a method of designing a tooth surface with a controllable tooth surface mark was proposed to design a tooth surface mark according to the actual needs.

In reference [26], the formula for calculating the instantaneous contact ellipse of the VH-CATT cylindrical gear pair is derived when the tooth surface deformation is equal to 0.00632 mm. According to the influence of the modification parameters on the contact area, the cutter head inclination angle γ is the parameter that has the greatest influence on the instantaneous contact ellipse. Therefore, the optimisation of the controllable design of the tooth surface mark aimed only at the cutter head inclination angle, and the long axis of the instantaneous contact ellipse aimed only at that of the pitch circle. In the design of the tooth surface mark, the long axis of the instantaneous contact ellipse is set as expected value L_E, and Eq. (20) is constructed to obtain an expected cutter head inclination angle.

$$f(\gamma) = A_g(\gamma) - L_E \tag{20}$$

where $A_g(\gamma)$ is the long axis of the instantaneous contact ellipse at the pitch circle and it is a function of γ.

Fig. 8 shows the influence of the modulus and tooth line radius on the cutter head inclination angle, and the expected values L_E are equal to $^1/_4B$ and $^1/_6B$, respectively. From Fig. 8, it can be seen that the cutter head inclination angle decreases with a decrease in the expected value of the contact ellipse long axis, and the cutter head inclination angle decreases with a decrease in the modulus and an increase in the tooth line radius. In some cases, the controllable design of the tooth surface mark is even not required.



(*a*) $L_E = {}^1/_4B$ (*b*) $L_E = {}^1/_6B$

Fig. 8 Influence of modulus and tooth line radius on cutter inclination angle

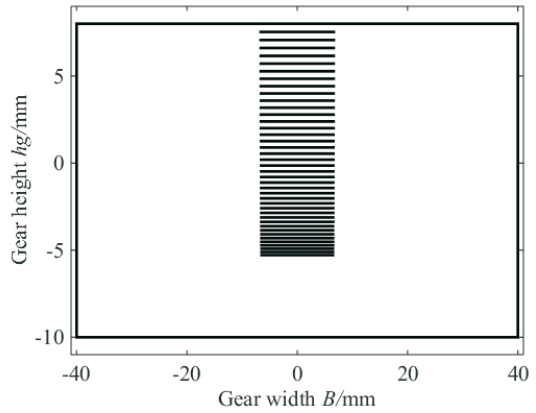


Fig. 9 Geometric contact trace of unmodified gear

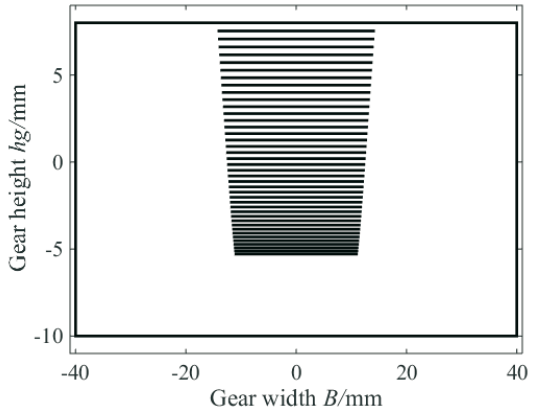


Fig. 10 Geometric contact trace of modified gear

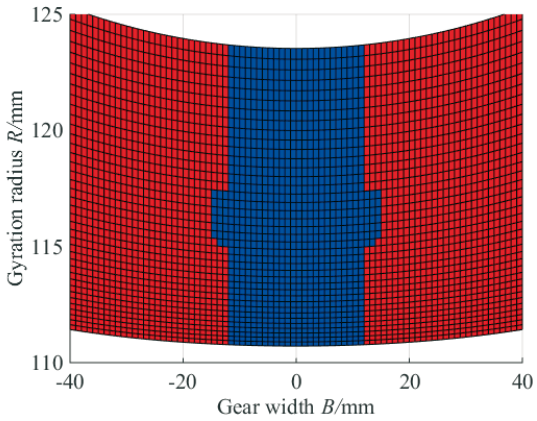


Fig. 11 Contact area of unmodified gear

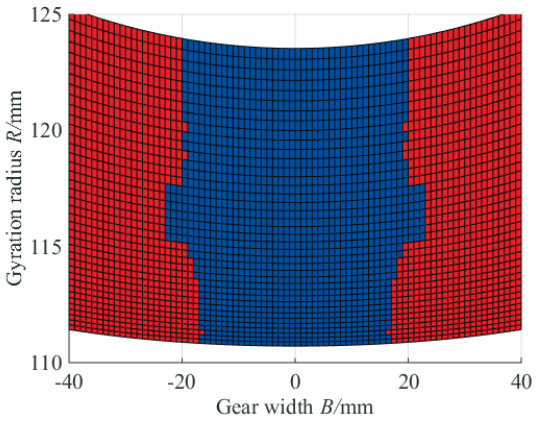


Fig. 12 Contact area of modified gear

In this paper, let the long axis of the instantaneous contact ellipse be about one sixth of the tooth width, the modulus m=8 mm, the tooth number ratio z_1/z_2=29/41, the tooth line radius R_T=200 mm, and the other parameters are the standard values. The cutter head inclination angle is calculated and rounded, and the cutter head inclination angle γ=6°.

Fig. 9 shows the geometric contact trace of the unmodified gear, while Fig. 10 shows the geometric contact trace of the modified gear. It can be seen that the contact trace of the unmodified gear is smaller than that of the modified gear, and the contact trace of the modified gear is about one third of the tooth width. The data shows that the expectation of the modification target is achieved. Also, an LTCA model is used to calculate the load-bearing contact area. The contact area is selected according to the standard that the contact force is greater than 0, the blue area being the contact area in the figure. Fig. 11 shows the contact area of the unmodified gear. Fig. 12 shows the contact area of the modified gear. From the figure, it can be seen that the contact area increases after modification, but the contact area obtained by the LTCA is larger than that obtained by the geometric contact analysis because of the increase in tooth surface deformation.

4.2 Tooth surface optimisation model

LTE reflects the deviation between the actual meshing position and the theoretical meshing position of the gear under load. The research shows that LTE is the direct excitation of the gear pair vibration during the working process, and it is an important factor in generating vibration and noise. Therefore, the optimisation design of the tooth surface modification aiming

at the vibration and noise reduction can be transformed into the optimisation design of the tooth surface modification for the LTE. Usually, in the gear transmission system, when the LTE is constant, the gear does not vibrate, so the goal of the tooth surface modification design is to control the amplitude of the load transmission error (ALTE) within the minimum range in the working process. According to the controllable design of the contact mark, the cutter head inclination angle can increase the contact mark on the tooth surface and effectively reduce the LTE of the VH-CATT cylindrical gear pair. To reduce the LTE further, a method for optimising the design of the tooth surface modification based on the minimum amplitude of LTE is proposed, which takes the parabolic coefficient and the parabolic vertex position as the optimisation parameters. In addition, because the gear pair usually works under multiple working conditions, the multi-objective optimisation design method is used to express the objective function as the minimum change of the LTE amplitude under a series of loads. The specific objective optimisation function is as follows:

$$\begin{cases} F(\boldsymbol{x}) = \min \sum_{i=1}^{n} w_i \dfrac{ALTE_i(\boldsymbol{x})}{ALTE_{i0}} \\ ALTE_i(\boldsymbol{x}) = \max(LTE_i) - \min(LTE_i) \\ ALTE_{i0} = \max(LTE_{i0}) - \min(LTE_{i0}) \\ S.T. \quad \boldsymbol{x}_{lb} \le \boldsymbol{x} \le \boldsymbol{x}_{up} \\ i = 1, 2, \cdots, n \end{cases} \tag{21}$$

where i is the load number, LTE_{i0} is the LTE of the unmodified gear pair under a certain load, $ALTE_{i0}$ is the LTE amplitude of the unmodified gear pair under a certain load, LTE_i is the LTE of the modified gear pair under a certain load, $ALTE_i$ is the LTE amplitude of the modified gear pair under a certain load, $\boldsymbol{x}$ is the matrix for the modification parameters a and u_0, $\boldsymbol{x}_{lb}$ is the lower bound of the modification parameters, $\boldsymbol{x}_{up}$ is the upper bound of the modification parameters, $F(\boldsymbol{x})$ is the fitness function, w_i is the load weight coefficient, and $\sum_{i=1}^{n} w_i = 1$.

Genetic algorithm (GA) simulates phenomena of duplication, crossover, and mutation in natural selection and heredity, and the optimal result can be obtained by calculation. Therefore, the GA is used to solve Eq. (21) to output the best modification parameters. Fig. 13 shows the optimisation process of the LTE based on the genetic algorithm, and the above optimisation calculation is completed by using the MATLAB language.

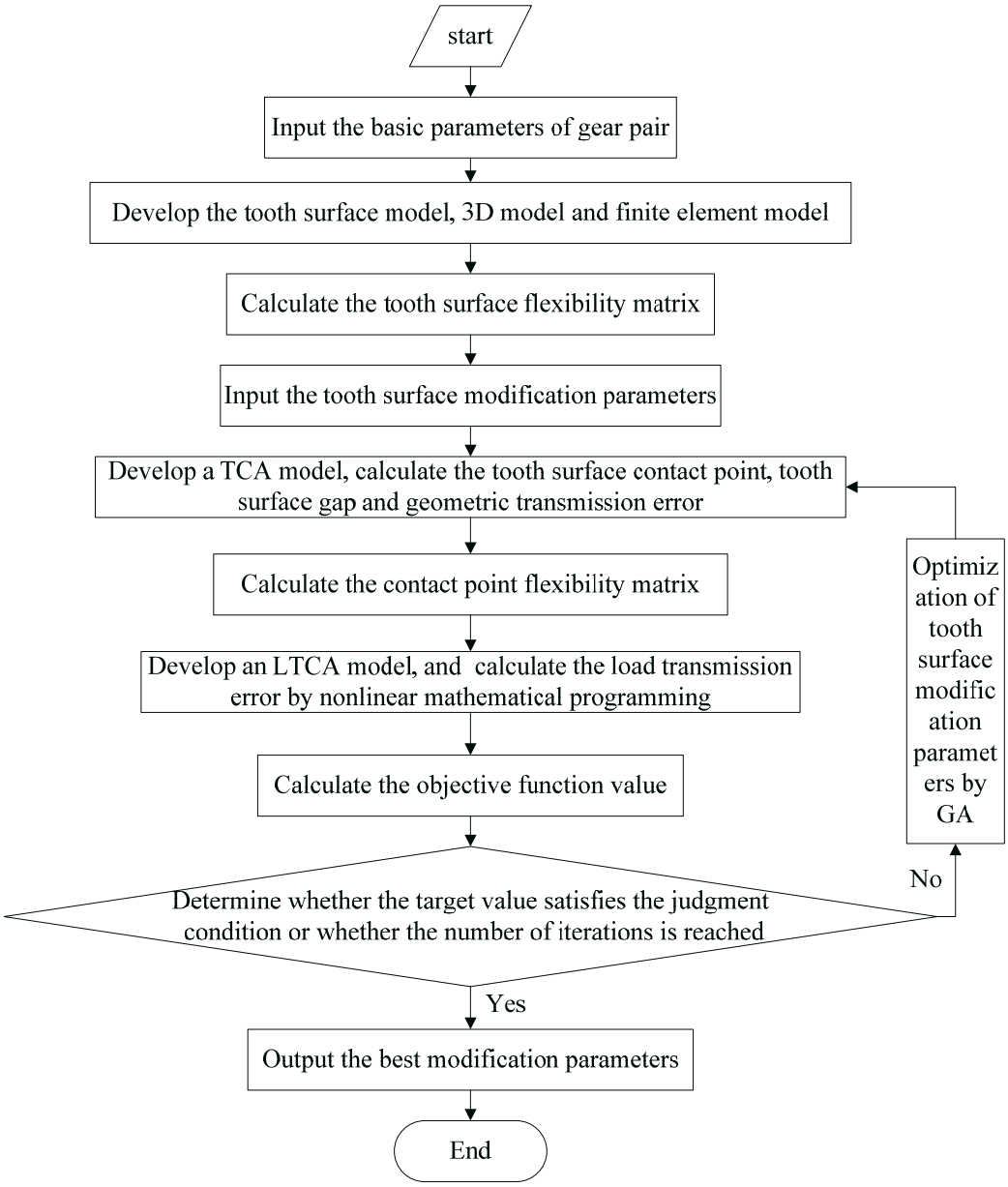


Fig. 13 Optimisation process of LTE based on genetic algorithm

4.3 Numerical example

Taking the following gear parameters: modulus m=8 mm, pressure angle α=20°, gear numbers z_1=29 and z_2=41, tooth line radius R_T=200 mm, and cutter head inclination angle γ=6°, a multi-objective optimisation design model was developed by using the MATLAB language and it was solved by the GA. The best value of the parabolic coefficient a is equal to 4.72×10^{-5}, and the best value of the parabola vertex position u_0 is equal to -1.18 mm.

Based on the optimal modification parameters, an LTCA model is developed to calculate the tooth surface load and the LTE. Fig. 14 shows the LTE of the unmodified VH-CATT cylindrical gear. Fig. 15 shows the LTE of the controllable design of the mark of the VH-CATT cylindrical gear. Fig. 16 shows the LTE of the comprehensive modification of the VH-CATT cylindrical gear. Fig. 17 shows the LTE of the three conditions, and M=1000 N·m. Fig. 18 shows the influence of the load on the LTE amplitude. It can be seen from Fig. 14 to Fig. 18 that the controllable design of the tooth surface mark can reduce the size and amplitude of the

LTE of the VH-CATT cylindrical gear. After the comprehensive modification of the parabolic blade, the size and amplitude of the LTE of the VH-CATT cylindrical gear reduce further. The LTE and the amplitude of the unmodified VH-CATT cylindrical gear and the VH-CATT cylindrical gear resulting from the controllable design increase with an increase in load. In the case of the VH-CATT cylindrical gear with parabolic blade comprehensive modification, the LTE of the VH-CATT cylindrical gear increases with an increase in load, but the LTE amplitude increases obviously with an increase in load only when the load is greater than 1000 N·m. At the same time, it can be seen that the LTE amplitude of the comprehensively modified VH-CATT cylindrical gear under light load is larger than that of the unmodified gear pair and the gear pair designed applying the controllable design of the tooth surface. The reason is that after the comprehensive modification the tooth surface gap increases, the geometric transmission error increases, and the system deformation increases.

Fig. 19 shows the load distribution of the unmodified VH-CATT cylindrical gear. Fig. 20 shows the load distribution of the tooth surface mark of the VH-CATT cylindrical gear designed by the controllable design. Fig. 21 shows the load distribution of the comprehensively modified VH-CATT cylindrical gear. From Fig. 19 to Fig. 21, that show a comparison with the unmodified gear, it can be seen that the tooth surface load of the contact mark achieved by the controllable design reduces and the contact area of the tooth surface increases. The tooth surface load of the comprehensively modified VH-CATT cylindrical gear reduces further, and the contact area of the tooth surface increases further.

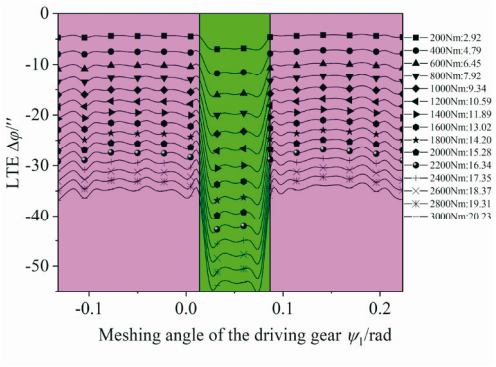


Fig. 14 LTE of unmodified VH-CATT cylindrical gear

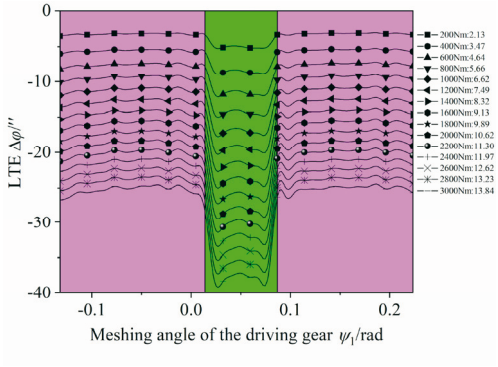


Fig. 15 LTE of mark of VH-CATT cylindrical gear achieved by controllable design

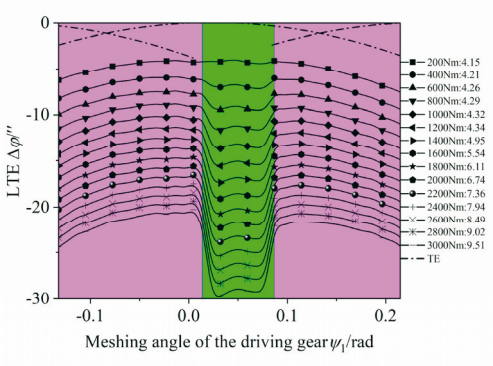


Fig. 16 LTE of comprehensively modified VH-CATT cylindrical gear

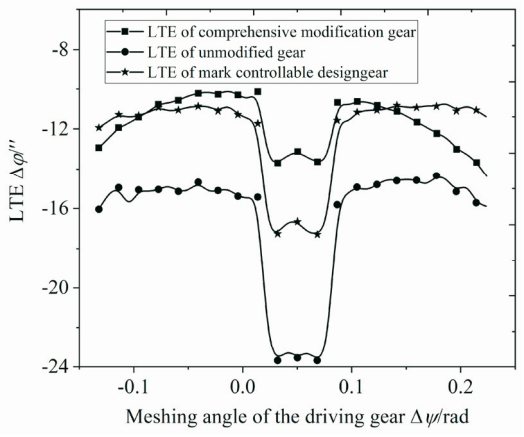


Fig. 17 LTE of three conditions (M=1000 N·m)

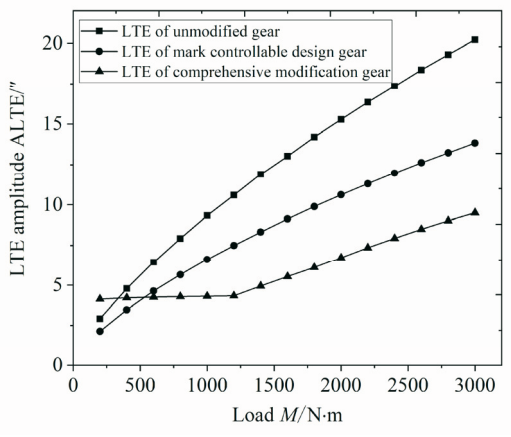
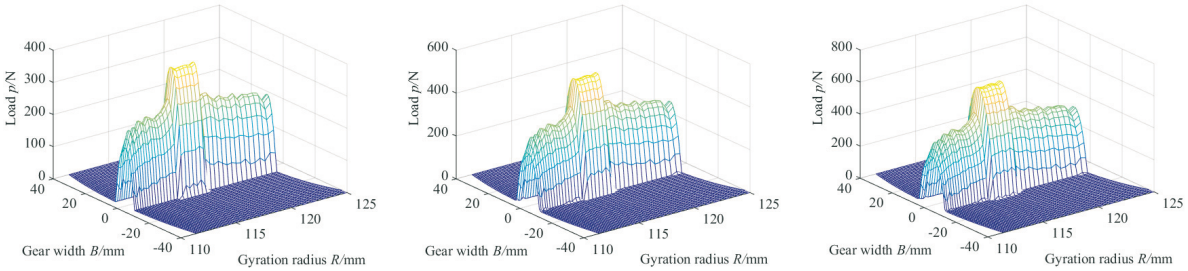
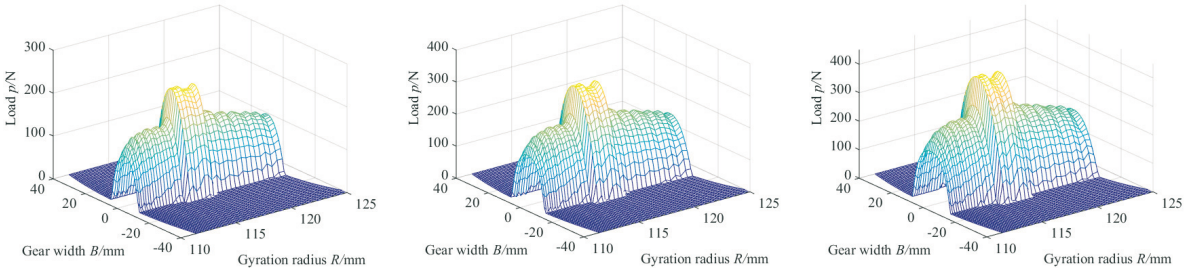


Fig. 18 Influence of load on LTE amplitude



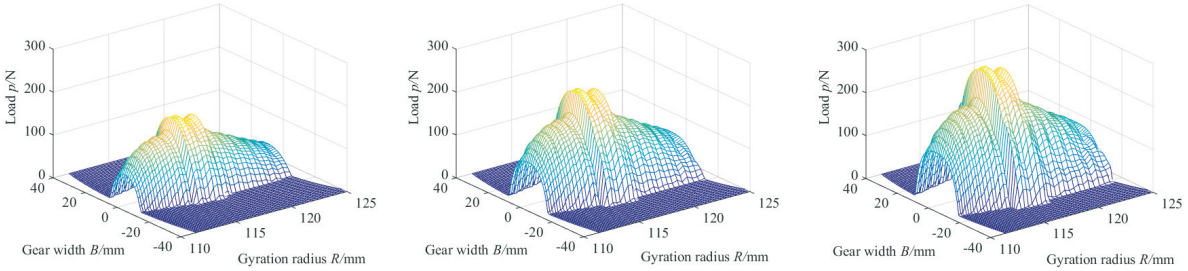
(*a*) M=600 N·m (*b*) M=1000 N·m (*c*) M=1400 N·m

Fig. 19 Load distribution of unmodified VH-CATT cylindrical gear



(*a*) M=600 N·m (*b*) M=1000 N·m (*c*) M=1400 N·m

Fig. 20 Load distribution of tooth surface mark of VH-CATT cylindrical gear designed by the controllable design



(*a*) M=600 N·m (*b*) M=1000 N·m (*c*) M=1400 N·m

Fig. 21 Load distribution of comprehensively modified VH-CATT cylindrical gear

5. Experiments

To verify the effect of the controllable design of the tooth surface mark and the tooth surface optimisation design of the vibration and noise reduction, the VH-CATT cylindrical gear reducer is processed and the tooth surface mark and transmission error experiment are carried

out. The main parameters of the VH-CATT cylindrical gear reducer are shown in Table 1. Fig. 22 shows the VH-CATT cylindrical gear reducer.

To test the meshing condition of the tooth surface and the contact area change of the tooth surface before and after the modification, the red powder was applied to the tooth surface of the reducer's driven gear, and the test system of the reducer was started to make the reducer rotate forward and reverse for a certain time, while the contact area of the tooth surface was observed. Fig. 23 shows the tooth surface mark of the modified VH-CATT cylindrical gear, while Fig. 24 shows the tooth surface mark of the unmodified VH-CATT cylindrical gear. It can be seen that the contact area of the VH-CATT cylindrical gear pair is extended to a line contact within a certain tooth width range in the actual test and work, and the gear contact area is in the middle area of the tooth width. The tooth surface contact area of the unmodified VH-CATT cylindrical gear pair is smaller than that of the modified VH-CATT cylindrical gear pair, and the contact area of the concave and convex tooth surfaces is the same. The experimental results are consistent with the theoretical analysis of the influence of the modification parameters on the contact area. It can be concluded that the tooth surface forming method proposed in this paper can increase the tooth surface contact area of the VH-CATT cylindrical gear pair and improve the bearing capacity of the VH-CATT cylindrical gear pair.

Table 1 Main parameters of VH-CATT cylindrical gear reducer

Parameter	Numerical value	Parameter	Numerical value
Modulus m/mm	8	Tooth line radius R_T/mm	200
Gear numbers z_1 and z_2	21, 29	Parabolic coefficient a	$\pm 5 \times 10^{-5}$
Gear width B/mm	80	Parabola vertex position u_0/mm	0
Pressure angle α/°	20	Cutter head inclination angle γ/°	6

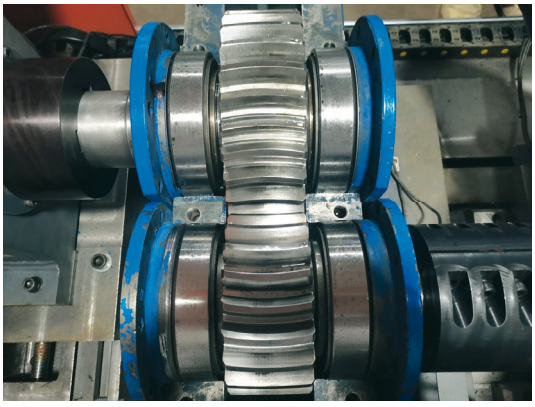


Fig. 22 VH-CATT cylindrical gear reducer

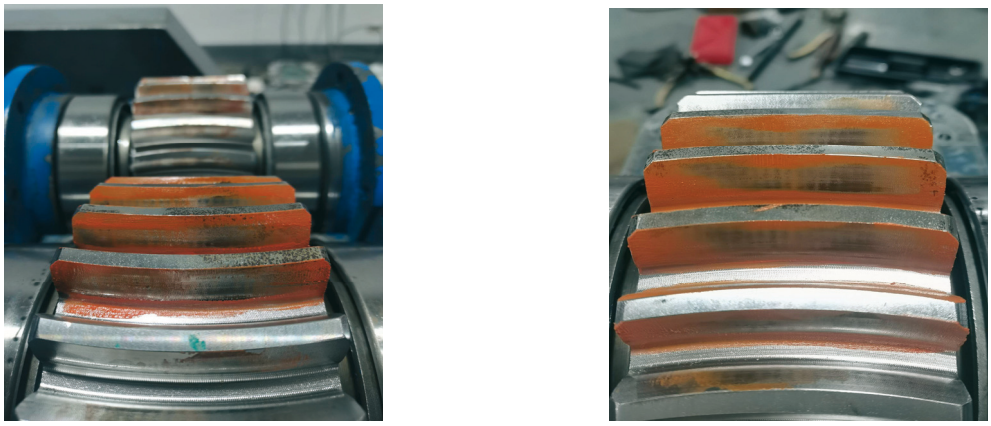


Fig. 23 Tooth surface mark of modified VH-CATT cylindrical gear



Fig. 24 Tooth surface mark of unmodified VH-CATT cylindrical gear

Fig. 25 shows a platform for testing the VH-CATT cylindrical gear reducer performance. It was used to measure the transmission error of the VH-CATT cylindrical gear reducer. In the experiment, the difference between the theoretical output angular displacement and the actual output angular displacement is defined as the system transmission error as follows:

$$TEa = \frac{\theta_{tp}}{i} - \theta_{tg} \tag{22}$$

where i is the transmission ratio, θ_{tp} is the actual rotation angle of the driving gear, and θ_{tg} is the actual rotation angle of the driven gear.

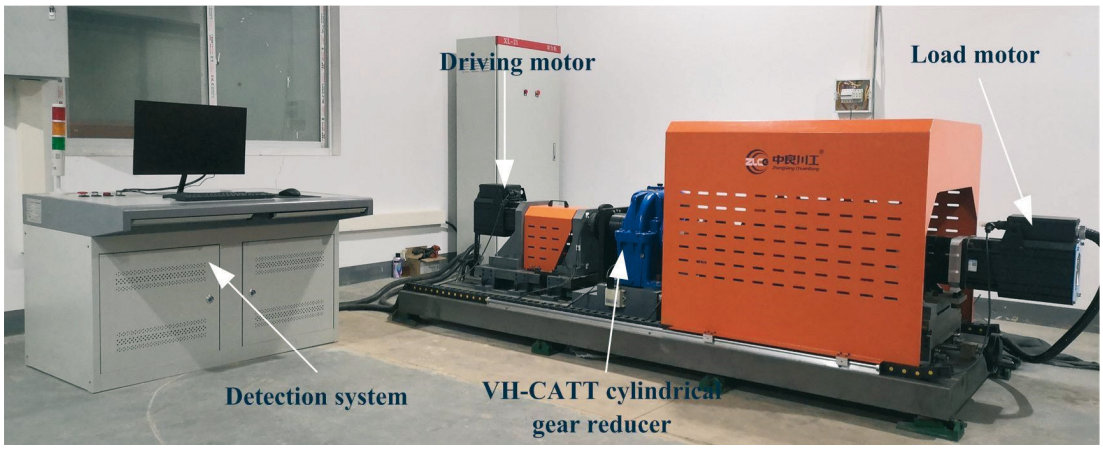
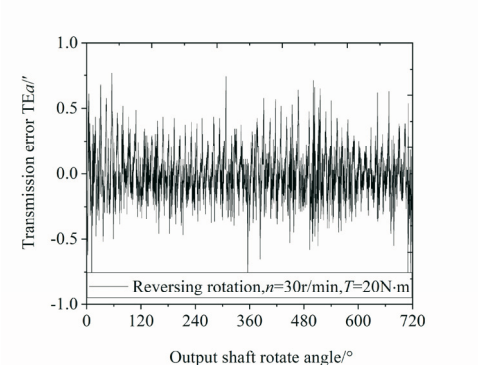
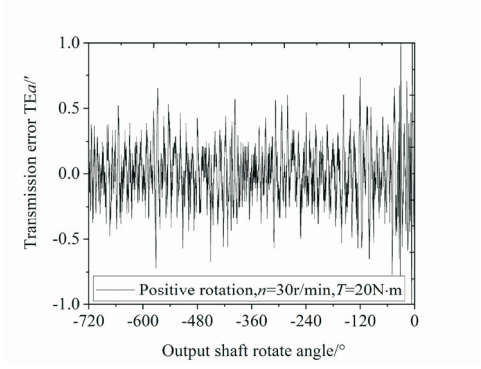


Fig. 25 VH-CATT cylindrical gear reducer performance test platform

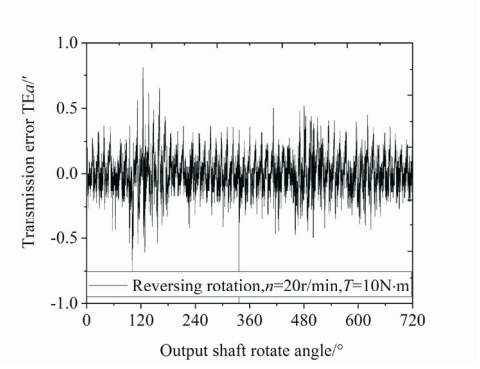
The experimental platform measures the actual rotation angle of the input and output shaft when the rotation is positive and reverse. The transmission error of the gear transmission system is calculated by Eq. (22). The experimental test is stopped when the output shaft rotates 720°. Fig. 26 shows the transmission error of the modified gear pair, while Fig. 27 shows the transmission error of the unmodified gear pair. The input speed n is 30 r/min and 20 r/min, and the load torque T is 20 N·m and 10 N·m, respectively. From the figures, it can be seen that the transmission error of the unmodified gear pair system fluctuates more than that of the modified gear pair system, and the transmission error distribution of the modified gear pair system is basically near the 0 line. The experimental results are consistent with the theoretical analysis of the trend of change of the transmission error, and there are only some differences in the values, which are related to the gear system load. The experiment shows that the modified gear pair has certain advantages, and the tooth surface modification is beneficial in reducing vibration and noise of the VH-CATT cylindrical gear.



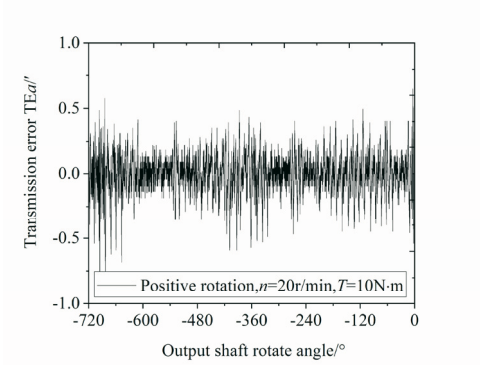
(a) Reverse rotation, n=30 r/min, T=20 N·m



(b) Positive rotation, n=30 r/min, T=20 N·m

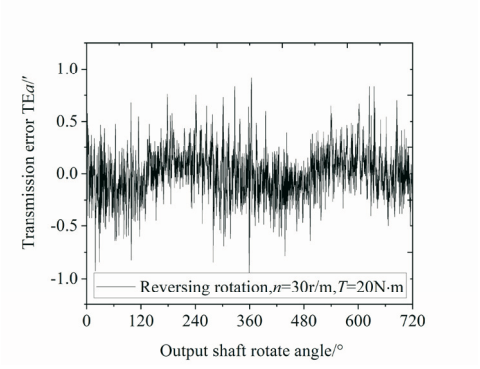


(c) Reverse rotation, n=20 r/min, T=10 N·m

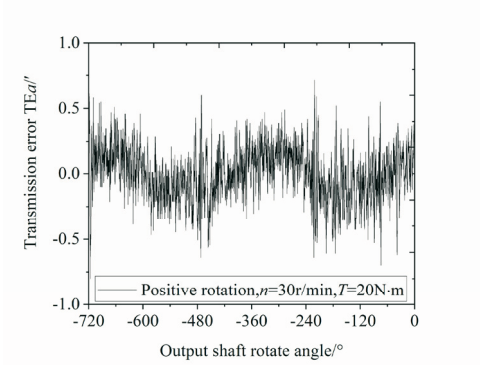


(d) Positive rotation, n=20 r/min, T=10 N·m

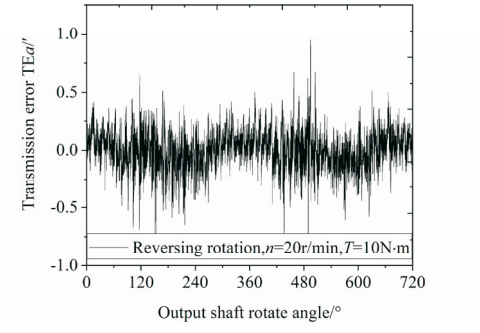
Fig. 26 Transmission error of modified gear pair



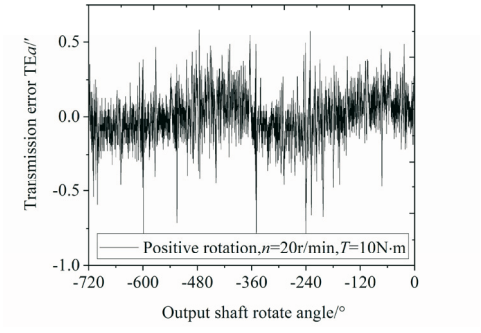
(a) Reverse rotation, n=30 r/min, T=20 N·m



(b) Positive rotation, n=30 r/min, T=20 N·m



(c) Reverse rotation, n=20 r/min, T=10 N·m



(d) Positive rotation, n=20 r/min, T=10 N·m

Fig. 27 Transmission error of unmodified gear pair

6. Conclusion

This paper discusses a design optimisation of the tooth surface of the VH-CATT cylindrical gear based on load transmission error. Firstly, a method for modifying the tooth surface with an inclined milling cutter head and a parabolic cutter blade was proposed based on the improvement in gear bearing capacity and reduction in meshing impact, and the modified tooth surface equation was derived. Next, an analysis model of the tooth contact of the VH-CATT cylindrical gear was developed to calculate the tooth surface gap, and a method for calculating the flexibility matrix was given based on the finite element and interpolation computation. An analysis model of the load tooth contact of the VH-CATT cylindrical gear was developed to calculate the load distribution and LTE. Then, a controllable design of the tooth surface mark was proposed to calculate the best inclination angle, and a tooth surface optimisation model was developed to calculate the best blade modification parameters. Finally, the tooth surface mark and transmission error experiments were carried out to verify the effect of the controllable design of the tooth surface mark and the tooth surface optimisation design of the vibration and noise reduction. The main conclusions can be expressed as follows:

(1) The surface load of the modified gear decreases and the load mutation in the alternate area of single and double tooth meshing also decreases. Further, the LTE increases at the moment of meshing-in and out, but the LTE amplitude and the LTE amplitude mutation in the alternating area of the single and double teeth meshing decrease.
(2) The contact area increases when the controllable design of the tooth surface mark is applied. The cutter head inclination angle decreases with a decrease in the expected value L_E, and it also decreases with a decrease in the modulus and an increase in the tooth line radius.
(3) The controllable design of the tooth surface mark can reduce the LTE size and amplitude. The LTE size and amplitude of the VH-CATT cylindrical gear are reduced after the comprehensive modification of the parabolic blade. The LTE and the amplitude of the VH-CATT cylindrical gear increase with an increase in load. The LTE amplitude of the comprehensively modified VH-CATT cylindrical gear under light load is larger than that of the gear pair that was not modified and the gear pair whose tooth surface was designed applying the controllable design.
(4) The experiment shows that the modified gear pair has certain advantages and the tooth surface modification is beneficial in reducing the vibration and noise of the VH-CATT cylindrical gear transmission system.

Acknowledgements

This study was supported by the Zunyi Normal University Doctor Fund (Zunshi BS [2024] 03Hao) and Zunyi Science and Technology Plan Project (Zunshikehe HZ Zi [2024] 139Hao).

Symbols and abbreviations

P_b	Normal pitch	ψ_1	Meshing angle of the driving gear
R_T	Tooth line radius	ψ_2	Meshing angle of the driven gear
γ	Cutter blade deflects angle	$\boldsymbol{r}_g^1$	Driving gear tooth surface
R_w	Gyration radius of the outer cutter blade on the node line	$\boldsymbol{r}_g^2$	Driven gear tooth surface
R_n	Gyration radius of the inner cutter blade on the node line	$\boldsymbol{n}_g^1$	Normal vector of the driving gear tooth surface
α	Gear pressure angle	$\boldsymbol{n}_g^2$	Normal vector of the driven gear tooth surface

O_{dp}	Parabola vertex position of the parabolic modification curve	$\boldsymbol{r}_g^m$	Position vector of the contact point
u_0	Distance between the parabola vertex position and the pitch line of the unmodified straight blade	$\boldsymbol{n}_g^m$	Common normal vector
a	Parabolic coefficient	$\boldsymbol{E}_M\boldsymbol{G}_M$ ($\boldsymbol{\xi}_e$)	Direction vector of the contact ellipse long axis
n	Parabolic order or input speed	φ_{110}	Initial angular displacement of the driving gear
v	Moving velocity of the inclined cutter head in the horizontal direction	φ_{11}	Angular displacement of the driving gear at a certain time
B	Gear width	z_1	Tooth numbers of the driving gear
R_1	Pitch circle radius	z_2	Tooth numbers of the driven gear
ω	Angular velocity of the cutter head	w	Gear tooth surface gap before loading deformation($w=b+$ ™)
ω_1	Gear blank's angular velocity	F_i	Equivalent load of the interpolation area points
m	Gear module of the VH-CATT cylindrical gear	$\boldsymbol{P}$	Tooth surface load
θ_d	Spreading angle of the cutter head	$[S]$	Flexibility matrix of the tooth contact point
φ_1	Involute angle of the tooth profile	$[F]$	Load matrix of the tooth contact point
Σ^{I}	Driving gear tooth surface	$[w]$	Initial clearance matrix
Σ^{II}	Driven gear tooth surface	$[d]$	Residual clearance matrix
M	Contact point of the tooth surface or load	$A_g(\gamma)$	Long axis of the instantaneous contact ellipse at pitch circle
T	Load torque	θ_{tp}	Actual rotation angle of the driving gear
i	Transmission ratio	θ_{tg}	Actual rotation angle of the driven gear
$\boldsymbol{n}_c$	Common normal vector of the contact point	VH-CATT	Variable hyperbolic circular arc tooth trace
TCA	Tooth contact analysis	LTCA	Load tooth contact analysis
LTE	Load transmission error	TE	Transmission error

REFERENCES

[1] Dias F., Silva G., Chui D. Vibration attenuation on spur gears through optimal profile modification based on an alternative dynamic model. Journal of the Brazilian Society of Mechanical Sciences and Engineering **2023**, 46, 10. https://doi.org/10.1007/S40430-023-04574-3

[2] Dong N., Zhou J., Tong R., et al. Study on the coupling relationship between wear and dynamics under steady uniform temperature field of planetary gear system. Journal of Mechanical Science and Technology **2023**, (12), 6405-6428. https://doi. org/10.1007/S12206-023-1114-1

[3] Mo S., Liu W., Tang X., et al. Research on nonlinear dynamics and primary resonance characteristics of electric drive gear transmission system for clean propulsion vehicles. Proceedings of the Institution of Mechanical Engineers Part K: Journal of Multi-body Dynamics **2023**, 237(4), 617-638. https://doi.org/10.1177/14644193231199723

[4] Zou H., Wang S., Li F., et al. Improved algorithm of tooth surface topological modification and nonlinear dynamic analysis of herringbone gears. Mechanism and Machine Theory **2023**, 180, 105151. https://doi.org/10.1016/j.mechmachtheory.2022.105151

[5] Yuan B., Liu G., Yue Y., et al. A novel tooth surface modification methodology for wide-faced double-helical gear pairs. Mechanism and Machine Theory **2021**, 160, 104299. https://doi.org/10.1016/j.mechmachtheory.2021.104299

[6] Peng X., Han F., Qiao X., et al. Tooth surface active modification and edge contact analysis for face gear drives with helical pinion. Computer Integrated Manufacturing System **2020**, 26(11), 3040-3048. https://doi.org/10.13196/j.cims.2020.11.014

[7] Jia C., Fang Z., Yao L., et al. Tooth modification design for vibration reduction of involute helical gears considering experimental load spectrum. Journal Central South University **2021**, 52(9), 3184-3193. https://doi.org/10.11817/j.issn.1672-7207.2021.09.020

[8] Jiang J., Liu Z., Liu H. Dynamic anti-wear design and analysis for hypoid gears with Ease-off flank modification. Journal of Mechanical Engineering **2021**, 57(19), 155-164. https://doi.org/10.3901/JME.2021.19.015

[9] Wei Y., Li Z., Liu Y., et al. Geometric contact characteristics and sensitivity analysis of variable hyperbolic circular-arc-tooth-trace cylindrical gear with error theory considered. Journal Northwestern Polytechnical University **2022**, 40(3), 679-689. https://doi.org/10.1051/jnwpu/20224030679

[10] Ma D., Ye Z., Yang H. Tooth surface reconstruction and tooth profile geometric analysis of circular arc tooth trace cylindrical gears. Transactions of Famena **2019**, 43(1), 29-44. https://doi.org/10.21278/TOF.43103

[11] Ma D., Liu Y., Ye Z., et al. Analysis of the Tooth Surface Contact Area of a Circular-Arc-Tooth-Trace Cylindrical Gear under Load. Transactions of Famena **2021**, 45(1), 79-94. https://doi.org/10.21278/TOF.451018220

[12] Aznar A., Orzaez R., Perez I. Comparison of spur, helical and curvilinear gear drives by means of stress and tooth contact analyses. Meccanica **2017**, 52(7), 1721-1738. https://doi.org/10.1007/s11012-016-0515-y

[13] Wu Y., Lou P., Bai Q., et al. Modelling and analyzing of loaded meshing characteristics of cylindrical gear transmission with curvilinear-shaped teeth. Meccanica 2023, 58(8), 1555-1580. https://doi.org/10.1007/S11012-023-01690-1

[14] Tseng R., Tsay C. Mathematical model and undercutting of cylindrical gears with curvilinear shaped teeth. Mechanism and Machine Theory **2001**, 36(11), 1189-1202. https://doi.org/10.1016/S0094-114X(01)00049-0

[15] Tseng R., Tsay C. Mathematical model and surface deviation of cylindrical gears with curvilinear shaped teeth cut by a hob cutter. ASME Journal Mechanical Design **2005**, 127(5), 782-987. https://doi.org/10.1115/1.1876437

[16] Tseng R., Tsay C. Undercutting and contact characteristics of cylindrical gears with curvilinear shaped teeth generated by hobbing. AMSE Journal Mechanical Design **2006**, 128(3), 671-680. https://doi.org/10.1115/1.2181605

[17] Dai Y., Yukinori A., Jiang D. Hobbing mechanism of cylindrical gear with arcuate tooth traces and experimental investigation. China Mechanical Engineering **2006**, 17(7), 706-709.

[18] Wu Y., Hou L., Luo L., et al. Research on the effect law of machine tool errors on tooth surface errors of curvilinear gear. Journal of Mechanical Engineering **2020**, 56(21), 100-109. https://doi.org/10.3901/JME.2020.21.100

[19] Wu Y., Hou L., Ma D., et al. Milling machine error modelling and analysis in the machining of circular-arc-tooth-trace cylindrical gears. Transactions of Famena **2020**, 44(1), 13-29. https://doi.org/10.21278/TOF.444009419

[20] Ma Z., Deng C. CNC machining method of whole modified surface of cylindrical gears with arcuate tooth trace. Journal of Mechanical Engineering **2012**, 48(5), 165-171. https://doi.org/10.3901/JME.2012.05.165

[21] Zheng F., Han X., Lin H., et al. Design and manufacture of new type of non-circular cylindrical gear generated by face-milling method. Mechanism and Machine Theory **2018**, 122, 326-346. https://doi.org/10.1016/j.mechmachtheory.2018.01.007

[22] Wei Y., Guo R., Liu Y., et al. Analytical Calculation of the Tooth Surface Contact Stress of Cylindrical Gear with Variable Hyperbolic Circular Arc Tooth Trace. Symmetry **2020**, 12(8), 1318. https://doi.org/10.3390/SYM12081318

[23] Wei Y., Yang D., Guo R., et al. Integrated wear prediction model for cylindrical gear with variable hyperbolic circular arc tooth trace under mixed elastohydrodynamic lubrication. Journal of Mechanical Science and Technology **2022**, 36(8), 4053-4065. https://doi.org/10.1007/s12206-022-0726-1

[24] Zhao F., Hou L., Duan Y., et al. Research on the forming theory analysis and digital model of circular arc gear shaped by rotary cutter. Journal Sichuan University **2016**, 48(6), 119-125. https://doi.org/10.15961/j.jsuese.2016.06.017

[25] Zhao F., Hou L., Chen Y., et al. Mathematical model and generating condition analysis of cylindrical gear with circular-arc-tooth-trace. Journal Jilin University **2020**, 50(3), 875-885. https://doi.org/10.13229/j.cnki.jdxbgxb20190058

[26] Liu Y., Ma D. Surface modification and tooth contact analysis of variable hyperbolic circular-arc-tooth-trace cylindrical gears. Mechanical Sciences **2022**, 13(2), 909-920. https://doi.org/10.5194/ms-13-909-2022

[27] Ma D., Liu Y., Ye Z., et al. Modification design and load tooth contact analysis of a cylindrical gear with variable hyperbolic circular arc tooth trace. Journal Vibration and Shock **2023**, 42(14), 170-179.

[28] Guo R., Wei Y., Liu Y., et al. Analytical solution to contact characteristics for a variable hyperbolic circular-arc-tooth-trace cylindrical gear. Mechanical Sciences **2021**, 12(2), 923-932. https://doi.org/10.5194/ms-12-923-2021

[29] Ma Z., Wang X., Shen B. Real tooth contact analysis of the cylindrical gears with symmetrical arcuate tooth trace. Journal XI'AN Jiaotong University **2005**, 39(7), 722-725.

[30] Chen Y., Lo C. Contact stress and transmission errors under load of a modified curvilinear gear set based on finite element analysis. Proceedings of the Institution of Mechanical Engineers Part C Journal of Mechanical Engineering Science **2015**, 229(2), 191-204. https://doi.org/10.1177/0954406214532907

[31] Luo P., Wu Y., Liang S., et al. TEHL analysis of VH-CATT cylindrical gear transmission in elliptical contact considering time-varying parameters. Advances in Mechanical Engineering **2022**, 14(2), 905-919. https://doi.org/10.1177/16878132221081615

[32] Fuentes A., Orzaez R., Perez I. Computerized design, simulation of meshing, and finite element analysis of two types of geometry of curvilinear cylindrical gears. Computer Methods in Applied Mechanics and Engineering **2014**, 272(15), 321-339. https://doi.org/10.1016/j.cma.2013.12.017

[33] Sun Z., Hou L., Wang J., et al. Contact strength analysis of circular-arc-tooth-trace cylindrical gear. Journal of the Brazilian Society of Mechanical Sciences and Engineering **2016**, 38, 999-1005. https://doi.org/10.1007/s40430-014-0272-6

[34] Zhang X., Xie Y., Tan X. Design, meshing characteristics and stress analysis of cylindrical gears with Curvilinear tooth profile. Transactions of Famena **2016**, 40(1), 27-44

[35] Ma D., Wei Y., Ye Z., et al. Mesh contact impact of circular arc tooth traces cylindrical gears. Journal Vibration and Shock **2018,** 37(7), 123-131. https://doi.org/10.13465/j.cnki.jvs.2018.07.019

[36] Ma D., Liu Y., Ye Z. Meshing Contact Impact Properties of Circular Arc Tooth Trace Cylindrical Gear Based on Rotating Knife Dish Milling Process. Mathematical Problems in Engineering **2021**, 2021, 1-17. https://doi.org/10.1155/2021/8819818

[37] Litvin F. L. Gear geometry and applied theory. PTR Prentice Hall Press **1994**.

[38] Fang Z. Model and approach for loaded tooth contact analysis (LTCA) of gear drives. Journal of Mechanical Transmission **1998**, (2), 2-4+17+53. https://doi.org/10.16578/j.issn.1004.2539.1998.02.001

Submitted: 25.02.2024

Accepted: 12.7.2024

Dengqiu Ma*
School of Engineering and Technology, Zunyi Normal College, Zunyi, China
School of Mechanical and Electrical Engineering, Lanzhou University of Technology Lanzhou, China

Bing Jiang
School of Mechanical and Electrical Engineering, Lanzhou University of Technology, Lanzhou, China

Zhenhuan Ye
School of Engineering and Technology, Zunyi Normal College, Zunyi, China

Yongping Liu
School of Mechanical and Electrical Engineering, Lanzhou University of Technology, Lanzhou, China

*Corresponding author:
scumdq@163.com